frontiers | Frontiers in Marine Science

TYPE Original Research
PUBLISHED 27 July 2023
DOI 10.3389/fmars.2023.1239682

OPEN ACCESS

EDITED BY
Hector Nolasco-Soria,
Centro de Investigación Biológica del Noroeste (CIBNOR), Mexico

REVIEWED BY
Carlos Alfonso Alvarez-González,
Universidad Juárez Autónoma de Tabasco, Mexico
Jingjing Tian,
Chinese Academy of Fishery Sciences, China

*CORRESPONDENCE
Fulvio Gandolfi
fulvio.gandolfi@unimi.it

RECEIVED 13 June 2023
ACCEPTED 07 July 2023
PUBLISHED 27 July 2023

CITATION
Verdile N, Camin F, Chacon MA, Pasquariello R, Pavlovic R, Peggs D, Fontanillas R, Tandler A, Kortner TM, Bitan A, Brevini TAL and Gandolfi F (2023) Evaluation of rainbow trout (*Oncorhynchus mykiss*) organotypic intestinal platforms: cellular responses after long-term exposure to *in vitro* digested feed. *Front. Mar. Sci.* 10:1239682. doi: 10.3389/fmars.2023.1239682

Evaluation of rainbow trout (*Oncorhynchus mykiss*) organotypic intestinal platforms: cellular responses after long-term exposure to *in vitro* digested feed

Nicole Verdile[1], Federica Camin[1], Marcelo A. Chacon[2], Rolando Pasquariello[1], Radmila Pavlovic[3,4], David Peggs[5], Ramon Fontanillas[5], Amos Tandler[2], Trond M. Kortner[6], Amir Bitan[2], Tiziana A. L. Brevini[3] and Fulvio Gandolfi[1]*

[1]Department of Agricultural and Environmental Sciences, University of Milan, Milan, Italy, [2]National Center for Mariculture (NCM), Israel Limnological & Oceanographic Research Institute (IOLR), Eilat, Israel, [3]Department of Veterinary Medicine and Animal Sciences, University of Milan, Lodi, Italy, [4]Proteomics and Metabolomics Facility, Istituto di Ricovero e Cura a Carattere Scientifico (IRCCS) San Raffaele Scientific Institute, Milan, Italy, [5]Skretting Aquaculture Innovation, Stavanger, Norway, [6]Department of Paraclinical Sciences, Faculty of Veterinary Medicine, Norwegian University of Life Sciences, Ås, Norway

Reliable and predictive *in vitro* models would support the search for new raw materials that can improve current fish diets. We recently developed some rainbow trout (RT) intestinal cell-based organotypic platforms demonstrating that the platform type modulates the degree of cell differentiation achieved *in vitro* and here we studied whether such differentiation correlates with their response to a prolonged exposure to a diet rich in fish meal. We compared three options, seeding the RTpiMI and RTdiMI cell lines derived respectively from the proximal or the distal intestine on (1) the polyethylene terephthalate (PET) culture inserts ThinCert™ (TC); (2) the TC coated with RT fibroblasts embedded within Matrigel® (MMfb); and (3) the highly porous polystyrene scaffold Alvetex™ also populated with fibroblasts (AV). Platforms have been exposed for 21 days to increasing concentrations of feed pellets digested *in vitro* by gastric and intestinal RT enzymes (IVD). Cells exposed to culture medium without IVD in each platform were used as controls. TEER values became significantly higher than their respective controls in most culture conditions. At the end of culture, epithelial cells formed multilayers irrespective of cell line or platforms if exposed to IVD, but not in the controls. This proliferative activity followed a dose-dependent pattern in the AV, did not vary in MMfb, and was highly variable in the TC. Moreover, IVD induced the formation of a few goblet-like cells characterized by rounded vacuoles. In parallel, alanine aminopeptidase activity completely disappeared in the MMfb, significantly decreased in the AV, but did not change in TC. These changes suggest a de-differentiation of the enterocytes and their

partial differentiation towards the secretory lineages. Overall, the three platforms reacted differently to a pronged exposure to IVD: TC quenched most of the cell responses, MMfb generated overly sensitive reactions, while the AV react mostly in a dose-dependent manner possibly generating more physiological results.

KEYWORDS

aquaculture, rainbow trout, *in vitro* intestine, *in vitro* digestion, organo-typic culture, cell differentiation, intestinal cell lines, enterocytes

1 Introduction

The aquaculture industry is dedicating efforts to the identification of more sustainable feed combinations in order to reduce the pressure on the marine environment, to optimize fish farming efficiency, and to improve animal health (Bell et al., 2004; Caimi et al., 2020; Randazzo et al., 2021; Cardinaletti et al., 2022). The biological value of novel ingredients is tested through *in vivo* experimentation with extensive commodity assessment programs to foresee and evaluate their ultimate impact on the gastrointestinal system and the animal as a whole. However, such a search is time-consuming, is expensive, and requires many animals, generating ethical concerns related to their welfare. These limitations could be mitigated by the development of predictive *in vitro* models to be employed especially during the screening process (Løkka et al., 2022). In this scenario, cell models are increasingly becoming a relevant supplement to *in vivo* research. They display several benefits, including reduced usage of experimental animals, continuous analysis, limited variability, immediate evaluation, and a rapid identification of the final result (Jung and Kim, 2022).

To date, fish cell-based models are already used to study different biological processes and provide a substantial contribution in a variety of areas such as biomedical research, biotechnology, disease control, environmental toxicology, ecotoxicology, fish immunology, and virology (Wang et al., 2019; Goswami et al., 2022; Løkka et al., 2023). Moreover, fish cell lines easily adapt to a wide spectrum of temperature, are characterized by higher resilience to hypoxia conditions, and are easier to maintain for prolonged periods of time in culture compared to mammalian cell lines (Goswami et al., 2022). Therefore, their attributes make them an attractive starting material for developing a reliable *in vitro* system.

Although fish-derived cell lines can be potentially used as a simplified system to explore nutrient uptake mechanisms and their metabolisms, their implementation in the field of fish nutrition is still largely unexplored. More than 10 years ago, the first stable rainbow trout (*Oncorhynchus mykiss*) intestinal cell line (RTgutGC) has been established (Kawano et al., 2011). RTgutGC has been widely used to investigate the environmental contaminant metabolisms and the response of the fish gut's immune system (Minghetti et al., 2017). Lately, the same system has been also used to evaluate the effects of functional feed ingredients (Wang et al., 2019).

More recently, we established two other novel epithelial intestinal cell lines (RTpiMI and RTdiMi) derived, respectively, from the proximal and distal portions of the rainbow trout intestine. When cultivated on permeable supports, they generate a functional intestinal barrier *in vitro* (Pasquariello et al., 2021). In parallel, we developed a procedure for extracting a bio-accessible fraction from feed pellets that can be supplemented to the cells without compromising their functions (Pasquariello et al., 2023).

We previously demonstrated that RT intestinal cell lines remain incompletely differentiated and proliferate regularly when cultured in classical cell culture flasks. However, when cells are grown in organotypic platforms, they differentiate into matured enterocytes (Verdile et al., 2023). Based on morphological and functional parameters, we observed that the degree of differentiation was influenced by the platform used. Moving from seeding the epithelial cells onto the classical insert with a PET membrane to a PET insert coated with a layer of fibroblasts embedded in Matrigel® and finally to porous polystyrene scaffold (Alvetex™) populated with the same fibroblast cell line, intestinal cells acquired an increasing amount of the mature enterocyte features.

The aim of the present work is to determine if and how the different degree of differentiation induced by three organotypic platforms is reflected in the cell's response to a prolonged exposure to a complete rainbow trout diet rich in fish meal.

2 Materials and methods

2.1 Rainbow trout cell culture

Rainbow trout proximal (RTpiMI) and distal intestine (RTdiMI) epithelial cell lines were routinely cultured as recently described by Pasquariello et al. (2021). In brief, both were maintained and propagated in 75-cm^2 flasks in complete medium ($L15/C_5$) made of Leibovitz's L-15 medium with Phenol red, supplemented with 5% fetal bovine serum (FBS), 2 mM of L-glutamine, and 10,000 units/ml penicillin, 10 mg/ml streptomycin, and 25 μg/ml amphotericin B. A stable cell line of rainbow trout fibroblasts derived from the dermis (RTskin01) was propagated in the same medium but supplemented with 10% FCS ($L15/C_{10}$). All cell lines were maintained at 20°C under ambient atmosphere.

2.2 Extraction of the bio-accessible fraction from pelleted fish feed

One experimental diet rich in fish meal was formulated according to requirements and produced by extrusion in 3-mm pellet size at Skretting Aquaculture Innovation (Stavanger, Norway). Fish feed formulation and proximate composition are listed in Table 1. Fish feed pellets have been digested *in vitro* [*in vitro* digested feed (IVD)] with enzymes naturally extracted from the RT digestive system to simulate both gastric (1,500 U/ml of pepsin activity) and intestinal (100 U/ml of trypsin activity) digestion following the protocol that we recently described (Pasquariello et al., 2023). In brief, *in vitro* digestion has been performed following the procedure previously described (Brodkorb et al., 2019) with some adjustments. First, ground RT feed pellets were mixed with water (0.125 g/ml), and then to simulate the gastric (pH 4) and the intestinal (pH 8) digestion stages, feed pellets were sequentially exposed to stomach and intestinal enzymes at 20°C for 6 h each. To inactivate the remaining enzymatic activity, IVD was heat-inactivated at 90°C for 10 min. Thereafter, the insoluble fraction was removed by centrifuging digesta samples for 30 min at 15,000 *g*. The supernatant was collected and lyophilized for at least 24 h. In this set of experiments, any undissolved lipid component was removed.

2.3 *In vitro* digested feed resuspension

Lyophilized IVD fish feed was resuspended in serum free L-15 medium, mixed by inversion, and centrifuged at 15,000 *g* for 15 min in a refrigerated centrifuge. The aqueous phase was collected and sterilized with 0.22-µm syringe filters under a horizontal laminar flow hood. Undiluted IVD, consisting of RT feed (composition is listed in Table 1), at an initial concentration of 0.125 g/ml, enzyme extracts, and distilled water, was diluted in L-15/C10 medium to obtain a final IVD concentration ranging from 6% to 50%.

TABLE 1 Diet composition.

Ingredient	Control
Corn gluten	5.6
Wheat gluten	15.5
Faba bean meal	7.9
Sunflower meal	10.4
Wheat	9.0
Fish oil	8.0
Fish meal	34.9
Rapeseed oil	8.2
Vit/Min premix	0.7
Volume	100.0
Moisture, %	7.0
Crude protein, %	46.5
Crude fat, %	23.0
Starch, %	10.0
DE MJ/kg	19.9
DP g/kg	413.0

2.4 Cell seeding and culture onto cell-based organotypic platforms

Three bi-cameral platforms have been assembled as recently described (Verdile et al., 2023) with the only exception of the Alvetex™-based platform whose assembly procedure has been slightly modified to improve the supportive stromal cell layer as detailed below.

2.4.1 Cell culture inserts (TC)

RTpiMI or RTdiMI cells were seeded at a final density of 2.5×10^5 cells/cm^2 onto ThinCert™ (TC)-permeable polyethylene (PET) translucent filter supports (Greiner BioOne, Kremsmuster, Austria, ThinCert™, translucent, 0.4 µm pore size, cat. No. 665640).

2.4.2 Cell culture inserts coated with fibroblasts embedded in Matrigel® (MMfb)

RTskin01 fibroblasts (4×10^5/cm^2) were resuspended in 125 µl of the solubilized basement membrane matrix Matrigel® (Corning®, New York, USA, cat No. CLS354234) diluted 1:8 in serum-free L-15 medium and layered onto ThinCert™ PET membranes with a 3-µm pore size (Greiner BioOne, Kremsmuster, Austria, ThinCert™, cat. No. 665631). After 1 week, 2.5×10^5 RTpiMI or RTdiMI cells/cm^2 were seeded on the apical part.

2.4.3 Alvetex™ scaffold (AV)

RTskin01 fibroblasts (1×10^6 cells/well) were seeded also into the synthetic scaffolding Alvetex™ (AV, Reprocell, Orlando FL, USA, cat. No. AVP005-12), a highly porous polystyrene thick insert that allows for cellular infiltration and the co-culture of cell types from different origins. To generate a robust artificial stroma, additional fibroblasts have been added to the system at days 7 and 9 of culture. RTski01 fibroblasts were stimulated to synthesize collagen by adding 100 µg/ml ascorbic acid to the cell culture medium. At day 14, RTpiMI or RTdiMI epithelial cells (9×10^5 cells/well) were layered on the top and cultured using standard complete medium without ascorbic acid.

2.4.4 Establishment of an effective barrier *in vitro*

To evaluate cell growth and the establishment of an effective epithelial barrier, transepithelial electrical resistance (TEER) was checked to evaluate whether the platforms reached their respective TEER plateau value (day 10 for TC and day 21 for MMfb and AV post-epithelial cell seeding). In brief, TEER has been measured using an EVOM2 (World Precision Instruments, Berlin, Germany) epithelial Voltmeter equipped with STX1 (for TC and MMfb) or STX2 (for AV) electrodes. For each well, resistance was measured in the three opposites sides, and then the average was calculated. A

blank insert, without cells, was run as control. TEER value was calculated using the following formula:

$$\text{TEER value } (\Omega * \text{cm}^2) = (\text{Insert value} - \text{Blank insert value}) * \text{Insert surface area}$$

All cell-based organotypic systems were deemed ready for IVD exposure after they reached TEER plateau values.

2.5 Prolonged exposure to IVD

The response of each platform to a prolonged exposure to IVD has been compared taking into consideration functional and morphological parameters. To this purpose, IVD was resuspended in L15/C_{10} medium at increasing concentrations (6%, 12%, 25%, and 50%) and was replaced twice a week (Figure 1). Negative controls were cultured in L15/C_{10} without IVD. TEER was measured twice a week in accordance with cell medium replacement (with or without IVD).

2.6 Evaluation of cellular response after prolonged exposure to IVD

At the end of the experiment (after 21 days exposition), the effects of a prolonged IVD administration on cellular health, function, and response have been compared among the different platforms.

2.6.1 Apparent permeability (P_{app})

To perform apparent permeability (P_{app}) assays, 100 µl of 4 kDa fluorescein isothiocyanate-dextran, (FITC-dextran, Merck, Darmstadt, Germany, cat. No. FD4) dissolved in L15/C_{10} (100 µg/ml) was dispensed in the apical chamber. After 1, 15, 30, 60, and 120 min, 100 µl of solution was collected from the basolateral compartment and transferred to a black, flat bottom, 96-well plate. A standard curve was prepared diluting 4 kDa FITC-Dextran in serial concentration ranging from 0 to 100 µg/ml in order to transform the fluorimeter readings into the corresponding dextran quantity. Standards and samples were measured using a Synergy HT, BioTek fluorimeter (em/ex 485/528).

Finally, to calculate the apparent permeability, the following formula was applied:

$$P_{app}\ (\text{cm}*\text{s}) = \frac{\Delta Q}{\Delta t} * \frac{1}{C_0 * A}$$

where $\Delta Q/\Delta t$ is the permeation rate of the molecule (the slope of the curve described by the cumulative concentration at the analyzed timepoints); C_0 is the initial concentration in the donor compartment; and A is the surface area.

2.6.2 Alanine aminopeptidase enzymatic activity

To evaluate cellular functionality, alanine aminopeptidase (ALP) was detected in live cells following a previously established procedure (Ferruzza et al., 2012). In brief, inserts were washed

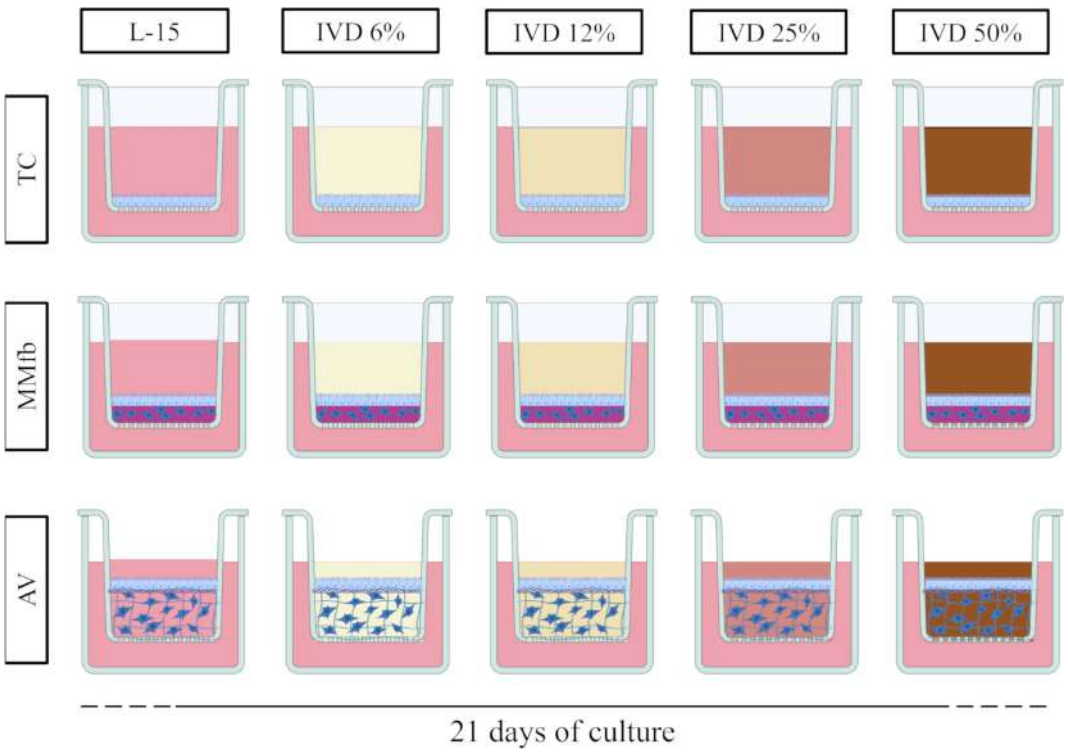

FIGURE 1
Schematic representation of the experimental design. TC, MMfb, and AV platforms were exposed for 21 days to increasing concentration of *in vitro* digested feed (6%, 12%, 25%, and 50%). For all platforms, controls were performed in parallel with L-15/C_{10} without IVD. Image created using BioRender.com.

thrice in PBS supplemented with 1 mM $CaCl_2$ and 1 mM $MgCl_2$ pH 7.0 (PBS^+). Samples were subsequently exposed to a solution of 5 mM L-alanine 4-nitroanilide hydrochloride diluted in 10 mM Tris-HCl and 150 mM NaCl, pH 8.0, in PBS. After 50 min, 100 µl of solution was collected from the apical compartment and transferred to a 96-well plate. A microplate reader was used to quantify the optical density at 405 nm (OD_{405}) (Bio-Rad, Hercules, CA, USA, microplate reader, Model 680). The standard curve was prepared from a 1 mM p-nitro anilide (p-NA) stock solution.

2.6.3 Histological histochemical and immunohistochemical analysis

At the end of the experiment, samples were fixed in 4% paraformaldehyde (PFA) overnight at 4°C, dehydrated, cleared in Histoclear (Histo-Line laboratories, Pantigliate, Italy, cat. No. R0050CITRO), and embedded in paraffin. Sections of 5-µm thickness were stained with hematoxylin and eosin or with 4′,6-diamidino-2-phenylindole (DAPI) to assess the general morphology of the cells cultured on the different inserts.

Other sections were stained for Periodic acid–Schiff (PAS) to highlight the presence of PAS-positive granules or vacuoles. A semi-quantitative scoring system has been applied to assess the frequency of their distribution in the different culture conditions as shown in Table 2.

The absence or the occurrence of a basement membrane has been indicated with "–" and "+", respectively.

Additional sections were used to detect proliferating cells. Actively diving cells were identified through indirect immunofluorescence. In brief, sections were brought to distilled water through sequential washings with xylene and ethanol at decreasing concentrations. Antigen retrieval was performed immersing slides in antigen retrieval solution (10 mM Tris-base, 1 mM EDTA solution, and 0.05% Tween 20, pH 9) in a pressure cooker for 1 min. Aspecific bindings were prevented by incubating slides in 10% goat serum in PBS for 30 min at room temperature (RT). Subsequently, specimens were incubated with mouse monoclonal anti-PCNA antibody (Merck, Darmstadt, Germany, cat. No. MAB424) diluted 1:1,200 in 4% BSA in PBS for 60 min at RT in a humid chamber. Thereafter, slides were incubated with the adequate secondary antibody Alexa Fluor™ 594 goat anti-mouse IgG 1:250 (Life Technologies Corporation, Willow Creek Road, OG, USA, cat. No. A11005) in PBS for 30 min. Sections were counterstained with 4,6-diamidino-2-phenylindole (DAPI) for 15 min and mounted with Pro-Long™ Gold Antifade Mountant (ThermoFisher Scientific, Waltham, MA, USA, cat. No. P36930).

TABLE 2 Semi-quantitative scoring system applied to evaluate the frequency of distribution of granules and vacuoles in PAS-positive sections.

Score	Description
–	Absence
+/–	Low frequency (1–3/slides)
+	Middle frequency (3/20 slides)
++	High frequency (>20 slides)

Secondary antibody controls were performed by omitting the primary antibody.

Pcna-stained sections were used to quantify the number of proliferating cells compared to epithelial cells in both experimental and controls samples. Briefly, three randomly selected fields of vision for each sample were selected, and all the visible nuclei and $Pcna^+$ cells were counted using the open-source software ImageJ (Schneider et al., 2012). For MMfb and AV platforms, which included both fibroblasts and epithelial cells, a line was manually traced to define the boundary between the two cell types so that only epithelial cells were counted. $Pcna^+$ cells have been expressed as a percentage of the total of the epithelial cells counted.

Images were acquired using a Leica DMR microscope equipped of a Nikon DS-Ri2 camera and the NIS-Elements D software, version 5.20.

2.7 Statistical analysis

Statistical analysis has been performed on IBM SPSS statistics (Version 28.0.0.1). Normal distribution and homogeneity of variances (homoscedasticity) were tested using Shapiro–Wilk test and Levene's test, respectively. Results were analyzed using one-way ANOVA followed by *post hoc* Tukey's test and are presented as mean ± standard deviation (SD). *p*-values of less than 0.05 were considered significant.

3 Results

3.1 Measurement of transepithelial electrical resistance

TEER values have been monitored twice a week along the 21 days of culture for each IVD concentration, platform, and cell line (Figure 2). IVD supplementation in the $L15/C_{10}$ medium showed a clear effect on TEER values. Indeed, at the end of the experiment, both RTpiMi and RTdiMI cells treated with IVD, irrespective of the platform, showed significantly higher TEER values compared to their respective controls exposed to the same medium but without IVD. However, in the TC and in the AV platforms, TEER value increased progressively with cell culture time. Moreover, the latter followed a dose–response effect, which was especially evident with the highest IVD concentrations. Conversely, in the MMfb system, the value increased sharply, right after a few days of culture to reach a plateau approximately 10 days post-IVD exposition. This result was observed even after low-dose IVD exposure (6 and 12%). The two cell lines followed approximately the same trend when cultured in the same platform.

3.2 Dextran apparent permeability (P_{app})

After 21 days of culture, the FD4 flux rate through the inserts covered by the epithelial barrier in all culture conditions (the different platforms cultured in combination with the two cell

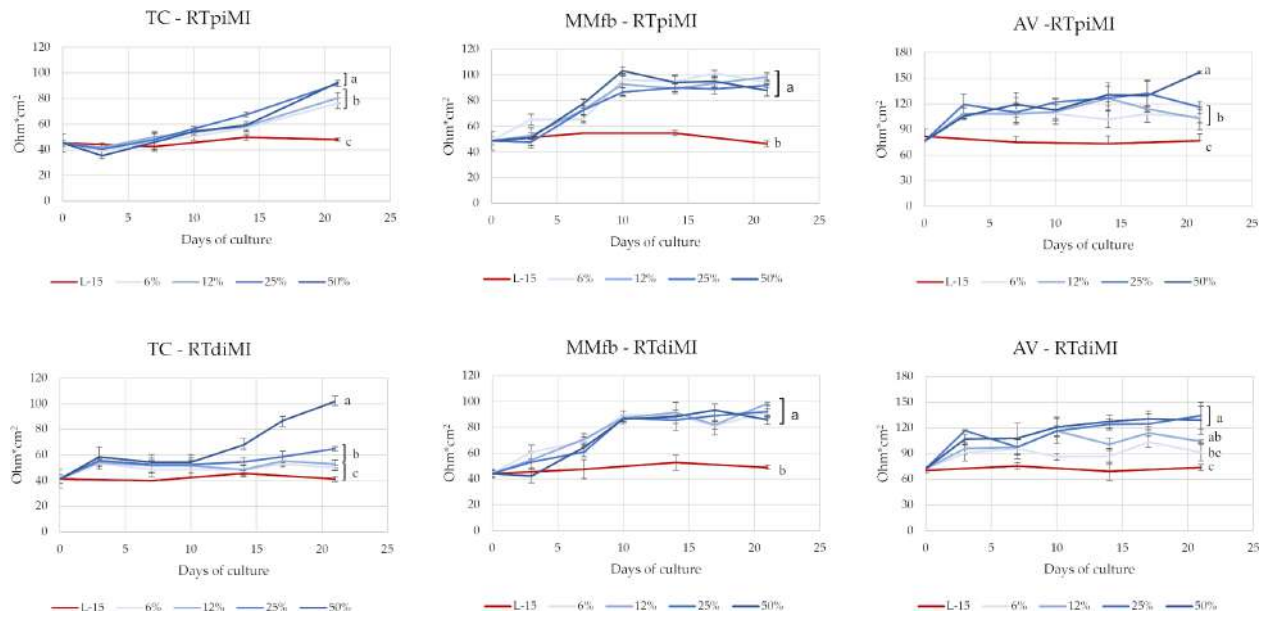

FIGURE 2
TEER values of RTpiMI and RTdiMI cells cultured in combination with TC, MMfb, or AV platforms during the 3-week exposure to IVD. Values are expressed as mean ± SD. (a-c) Different superscripts in the same graph indicate statistically significant differences ($p < 0.05$).

lines) was significantly slower than through the same inserts without cells. The FD4 flux rate through the TC and MMfb epithelial barrier became significantly slower than the controls (L-15/C_{10} medium) already at the lowest IVD concentration in both cell lines. In contrast, the FD4 flux through the epithelial barrier in the AV platform did not differ from the control event at the highest IVD concentration, again with no difference between cell lines (Figure 3).

3.3 Alanine aminopeptidase enzymatic activity

We evaluated the activity of ALP to determine whether the different IVD concentrations promoted cellular functionality and proteolytic digestion.

While IVD supplementation did not produce any effect on RTpiMI cells grown on TC, even low IVD concentrations resulted in a significant increase in the ALP activity in RTdiMI cells cultured in the same system. In the AV platform, cell lines reacted in a different but opposite way to IVD, which inhibited the ALP activity of RTpiMi cells but did not affect that the RTdiMI line. Finally, the MMfb platform induced a further different result completely inhibiting ALP activity from the lowest IVD concentration in both cell lines (Figure 4).

3.4 Histological and histochemical analysis

No morphological damages were visible in HE-stained sections, but a clear epithelial stratification was observed in all cultured conditions, irrespective of cell lines or platforms. Such changes were not observed in controls not exposed to IVD where cells remained in monolayer. Interestingly, in all platforms, the epithelial stratification followed a dose–response effect and was, therefore, highest after the administration of 50% IVD. At this concentration, the number of cells was so high that it induced the detachment of cell layers from the membrane surface.

In more detail, both epithelial cell lines had a flat, elongated shape when cultured on TC inserts with or without IVD (Figure 5). In the MMfb platform, some fibroblasts migrated through the porous membrane adhering to its basal side, when embedded in the Matrigel® matrix, a possible consequence of the membrane large pore size (3 μm) combined with the long culture time. In this platform, any IVD concentration induced a modification of the cell phenotype compared to the control, more evident in the RTdiMI cell line, in which the superficial epithelial layer assumed a cubic morphology. Furthermore, IVD led to the formation of well-defined vacuoles with a rounded shape and variable in size (Figure 6).

Also in the AV platform, IVD supplementation resulted in the formation of a pluristratified epithelium, which was particularly evident in RTdiMI cells with a clear dose response. Conversely, RTpiMI treated with 6% IVD mostly preserved the same monolayer of cubic cells observed in the control. As it happened in the MMfb platform, IVD induced the formation of visible vacuoles also in the AV, which were instead absent in the controls (Figures 7, 8).

PAS staining on paraffin sections revealed the presence of PAS-positive granules scattered in the epithelial cells' cytoplasm after IVD supplementation. Such granules were smaller in size compared to the vacuoles observed with HE and were once again absent in the respective controls. While they were limited in number in the TC, they were abundant in the MMfb and AV platforms. Moreover, in all conditions, they occurred more frequently in RTdiMI cells compared to RTpiMI (Figures 9A, B).

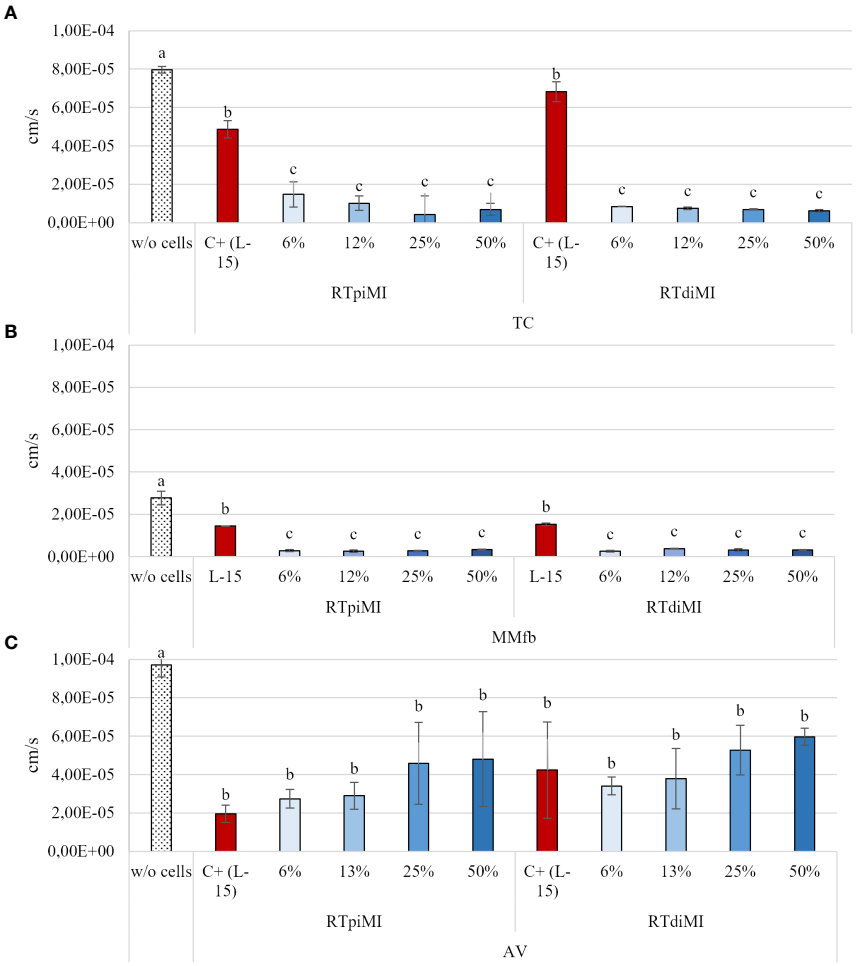

FIGURE 3
Apparent permeability of FD4 through the epithelial barriers formed in the TC **(A)**, MMfb **(B)**, and AV **(C)** platforms, measured after 21 days of exposure to increasing concentrations of IVD. Values are expressed as mean ± SD. (a-c) Different superscripts in the same graph indicate statistically significant differences ($p < 0.05$).

In addition, exposure to IVD resulted in the formation of a distinctive basement membrane between epithelial and connective cells in both MMfb and AV platforms. This acellular layer showed a strong affinity for PAS staining because of its high glycoprotein nature. A comparable structure was not seen in the TC platform either with or without IVD (Figure 9C). Finally, few vacuoles displaying high affinity for PAS staining were observed exclusively in the AV platform (Figure 10).

Results related to the semi-quantitative scoring system are shown in Table 3.

3.5 Immunohistochemistry

Proliferating cells were identified through immunodetection of Pcna specifically in the cell nucleus. Cell proliferation was estimated counting the proportion of $Pcna^+$ cells of the total of epithelial cells.

In general, the percentage of $Pcna^+$ cells found in the TC platform was variable and inconsistent among the different conditions generating high variability. This was caused by the low adhesive properties of the TC sections. While the percentage of $Pcna^+$ cells remained stable in MMfb, irrespective of IVD concentrations or cell line, the percentage of proliferating cells significantly increased compared to the controls in RTdiMI cultured in AV after the addition of high (25% and 50%) IVD doses (Figures 11, 12).

4 Discussion

We previously established that RT intestinal cell line differentiation is influenced by the organotypic platform upon which cells are grown (Verdile et al., 2023). Here, we evaluated whether and how the different degrees of differentiation induced by the platforms correlate with the cell response after a prolonged exposure to the bioactive fraction extracted from pellets of a complete diet with high levels of fish meal.

We used RTpiMI and RTdiMI intestinal cells lines derived from the rainbow trout proximal and distal intestine, respectively (Pasquariello et al., 2021), cultured on three organotypic cell-

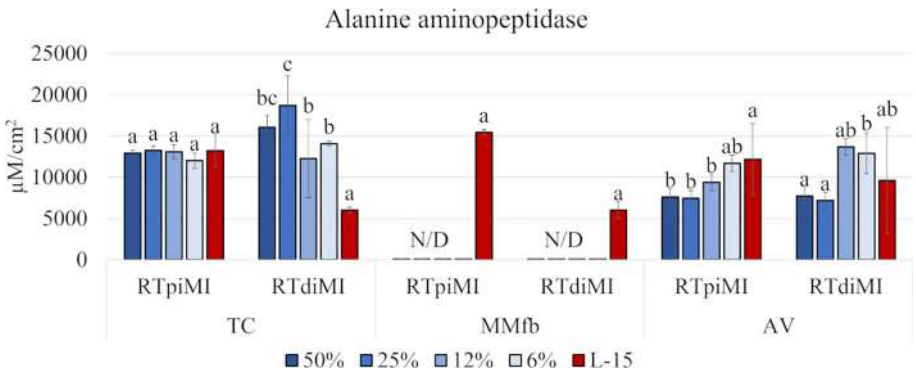

FIGURE 4
Bar charts showing the quantification of the alanine aminopeptidase (ALP) activity in RTpiMI and RTdiMI cells cultured in combination with TC, MMfb, and AV platforms after 21 days of exposure to increasing concentrations of IVD. Values are expressed as mean ± SD. Differences were considered statistically significant if $p < 0.05$. different letters within the same culture conditions (platform and cell line) indicate statistically significance differences. N/D indicates a non-detected value.

based platforms that we recently characterized (Verdile et al., 2023). For all our experiments, we used RT feed pellets with a high fish meal content, the classical reference diet used in feeding trials.

To obtain a prolonged exposure without compromising cell function, IVD has been continuously supplemented to the complete cell culture medium that was replaced twice a week. The establishment of a functional epithelial barrier has been used as the reference parameter for normalizing the time when IVD began to be administered to the different platforms. We considered that a functional epithelial barrier had formed when two consecutive measurements of the TEER gave non-significantly different results (Verdile et al., 2023). Being a non-invasive procedure, TEER value is an effective marker for monitoring changes during a prolonged *in vitro* experiment (Felix et al., 2021). Indeed, after the epithelial barriers were exposed to IVD, TEER values gradually increased above the plateau values in many culture conditions with some

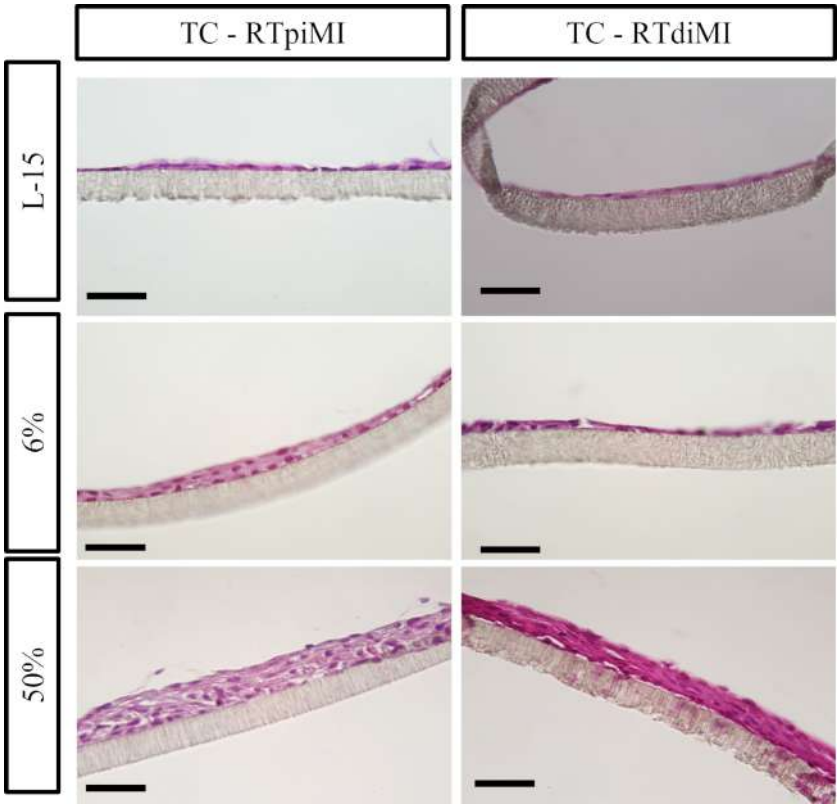

FIGURE 5
Representative HE-stained sections of the TC platform showing the formation of cellular multilayers after 21 days of chronic exposure to increasing concentrations of IVD. Epithelial cells have a flat and elongated morphology (scale bar, 50 µm).

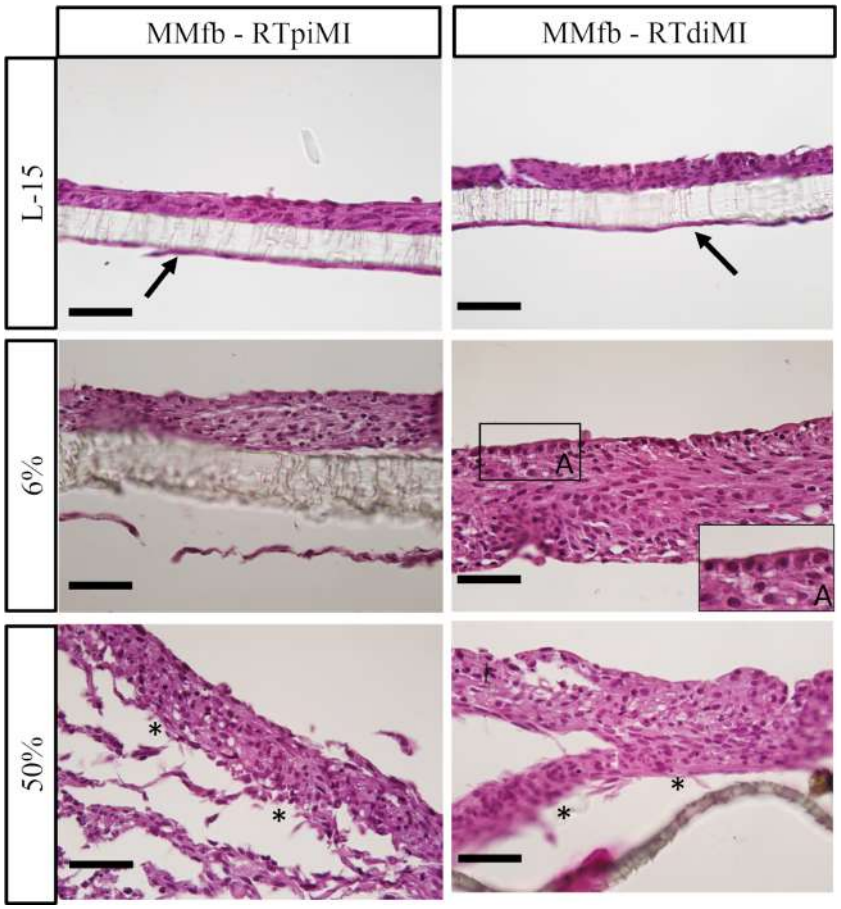

FIGURE 6
Representative HE-stained sections of the MMfb platform after 21 days of chronic exposure to increasing concentrations of IVD showing a gradual epithelial stratification. Fibroblasts migrating through the porous membrane adhering to its basal side are indicated with arrows; the cubic phenotype acquired by epithelial cells after IVD exposure is shown in the photomicrograph A. Asterisks indicate detachment of cell layers from the membrane at the highest IVD dose (scale bar, 50 µm).

variations depending on the combination of platform type, IVD concentration, and cell line. The MMfb platform somehow quenched all differences between cell lines and IVD treatments but amplified that of the IVD exposure compared to the control. In TC and AV platforms, the increase took place gradually, along the cell culture time and following a dose-dependent pattern but did not reach a plateau at the end of the treatment, suggesting that additional exposure to IVD could result in even higher TEER levels.

Measuring the apparent permeability of 4 kDa dextran across the epithelial barrier showed that the TEER increase observed in the TC and MMfb platforms was accompanied by a decrease of paracellular permeability. On the other hand, however, the same did not happen with the AV platform where neither the IVD concentration nor the cell line were able to influence paracellular permeability as opposed to TEER. This finding is consistent with our recent results (Verdile et al., 2023), indicating that TEER and paracellular permeability measured as 4 kDa dextran P_{app} are often unrelated since the two techniques measure an independent process (Bednarek, 2022).

No morphological damage was visible in HE-stained sections, but a clear epithelial stratification was observed in all culture conditions. Such epithelial remodeling was not observed in the controls not exposed to IVD where cells remained in monolayer. This observation leads us to exclude that the massive stratification is related to the extended time in culture. In addition, the fact that the epithelial stratification followed a dose-dependent pattern further supports the theory that the increase in epithelial cell layers was a direct result of the IVD administration. The increased number of cell layers can explain most of the increment in TEER values described above. Indeed, a recent study using the Caco2 cell line showed that changes of cell number and the consequent increase of junctional length determine a significant effect on TEER values (Felix et al., 2021).

IVD supplementation did not affect the morphology of cells cultured on TC that conserved the same flat and elongated shape observed in the controls. Conversely, in the MMfb, IVD seems to induce a better morphological organization of epithelial cells lining the upper surface that assumed a more cubic shape even after exposure to low IVD doses. Finally, in the AV platform, a cell monolayer made of well-polarized cells was partially preserved in RTpiMI after exposure to low IVD dose but was lost at the highest IVD concentration. Interestingly, we recently observed that after having been exposed to a nutritional challenging condition, the

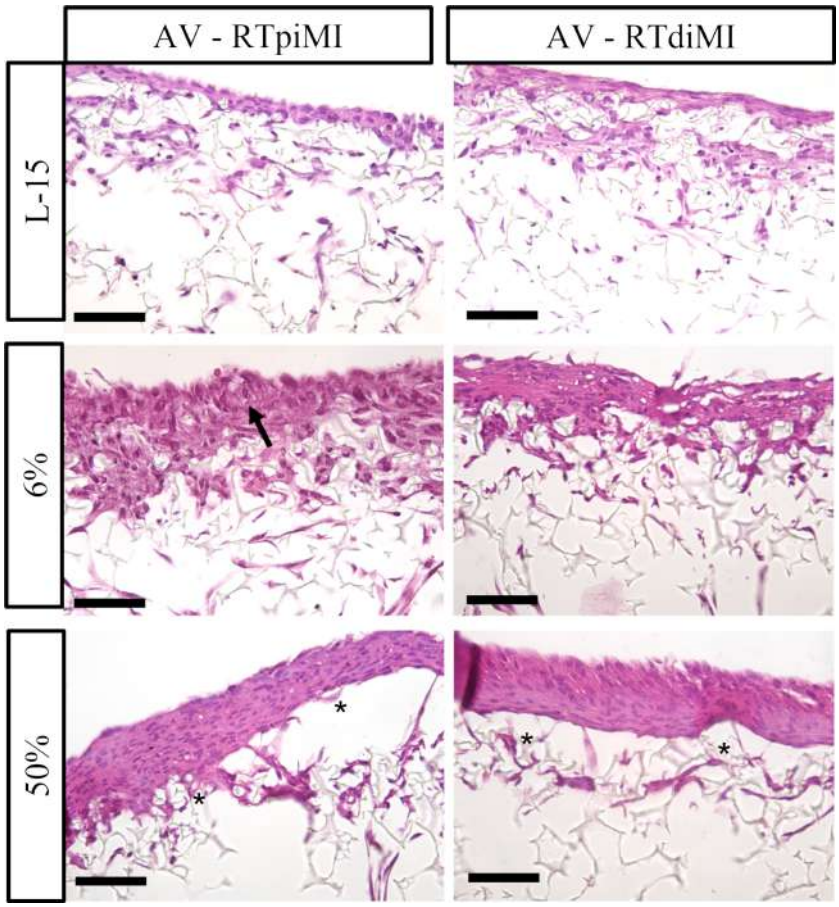

FIGURE 7
Representative HE-stained sections of the AV platform after 21 days of chronic exposure to increasing concentrations of IVD showing a clear epithelial stratification with a dose–response effect. The monolayer and polarized epithelium conserved in RTpiMI with 6% is indicated with arrow. Asterisks indicate cell layer detachment from the membrane surface after the highest IVD concentration (scale bar, 50 μm).

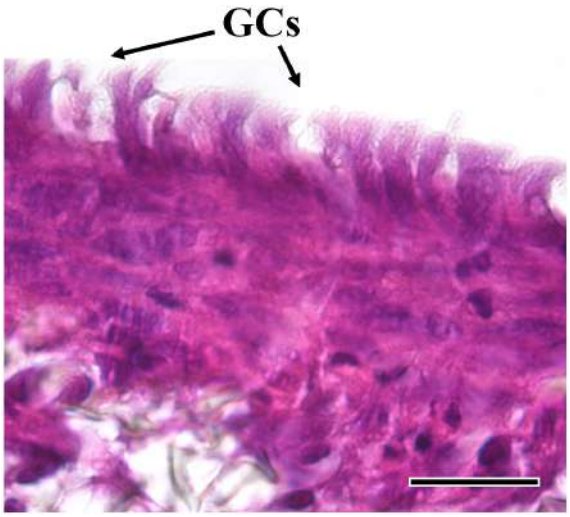

FIGURE 8
Representative HE-stained section of the AV platform cultured in combination with RTdiMI cell line after 12% IVD. Rounded shape vacuoles that show high similarity with goblet cells are found. (GCs: goblet-like cells) (scale bar, 25 μm).

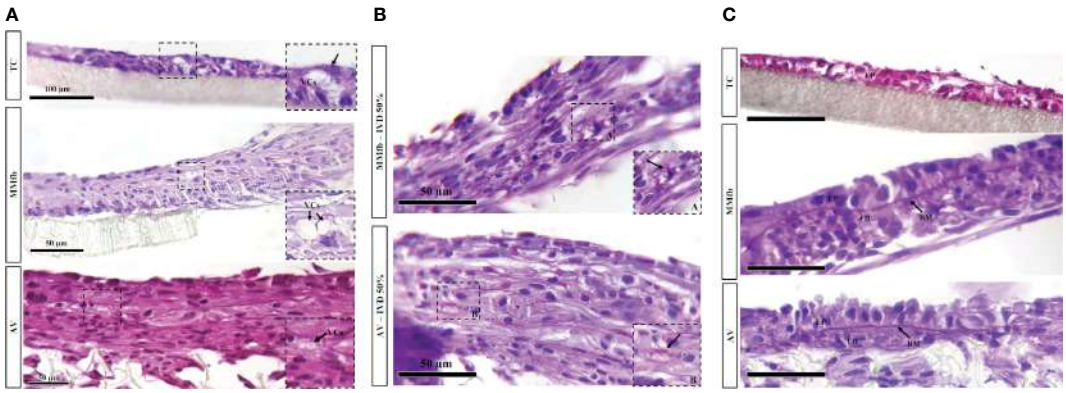

FIGURE 9
(A) Representative PAS-stained sections of TC, MMfb, and AV platforms after 25% IVD administration showing the presence of rounded well-defined vacuoles (VCs) having a variable size. **(B)** Representative PAS-stained section of MMfb and AV showing the presence of PAS-positive granules (arrows) in the epithelial cell cytoplasms. **(C)** Representative PAS-stained section of TC, MMfb, and AV showing the presence of distinctive basement membrane (MB) between epithelial (EP) and fibroblast (FB) cells after exposure to IVD. Such acellular layer was absent in TC platform (scale bar, 50 µm).

proximal RT intestine generated novel stem cell niches, presumably reverting their mature phenotype and creating new proliferating zone to mitigate the nutritional stress (Verdile et al., 2022). Therefore, we hypothesize that what we observed is something similar: the reaction to a nutritional stress in a rudimentary form. In fact, even if we used a non-challenging diet, the epithelium may have reacted because, *in vitro*, it is devoid of the natural protection provided by the mucus layer.

In this respect, it was interesting to observe, in all platforms, the appearance of cells presenting well-defined vacuoles rounded in shape and variable in size, which were absent in the controls. Based on their morphology, they could be ascribable to goblet-like cells. This suggests that IVD supplementation could stimulate epithelial cells to differentiate into mucus-secreting cells. Indeed, experimental data in mice showed that under inflammatory or pathological conditions, epithelial progenitors, responsible for the maintenance of the different cell types in the intestinal epithelium, are pushed to differentiate into secretory lineages including goblet cells instead of the absorptive cell population, to meet the gut mucosa requirements of the moment (Mahapatro et al., 2016; Kurashima et al., 2017). Given that we

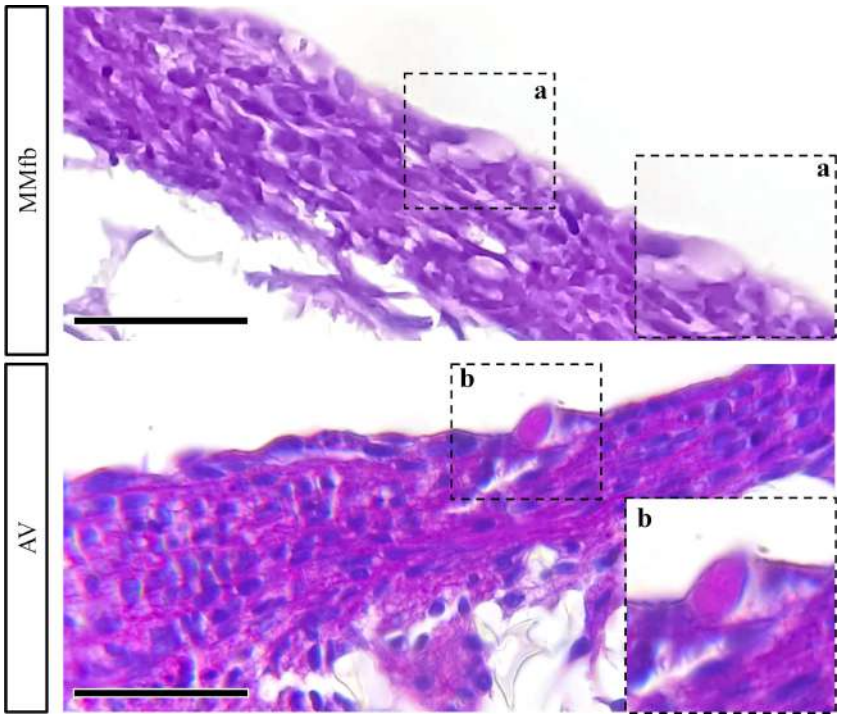

FIGURE 10
Representative PAS-stained section of MMfb and AV showing the presence of goblet-like cells (GCs) scattered among enterocytes like cells. Notably, only GCs found in the AV showed affinity for PAS (scale bar, 50 µm) (panel a and b represent photomicrographs of GCs at higher magnification).

10.3389/fmars.2023.1239682

TABLE 3 Semi-quantitative scoring system showing the distribution as well as the abundance of granules, vacuoles, and basement membrane in the different culture combinations (platforms and cell line).

		RTpiMI					RTdiMI				
		L-15	6%	12%	25%	50%	L-15	6%	12%	25%	50%
Granules	**TC**	–	+/–	+/–	+/–	+	–	+/–	+/–	+	+
	MMfb	+/–	+/–	+	+	+	+/–	+	+	+	++
	AV	+/–	+/–	+	+	+	+/–	+	+	++	++
Vacuoles	**TC**	–	+	+	+	++	–	–	+/–	+	+
	MMfb	–	+	+	+	++	–	+/–	+	+	+ +
	AV	–	–/+	+	++	++	–	+	+	+	++
Basal membrane	**TC**	–	–	–	–	–	–	–	–	–	–
	MMfb	–	+	+	+	+	–	+	+	+	+
	AV	–	–	+	+	+	–	+	+	+	+

– indicate absence, +/– indicate low frequency, + indicate middle frequency, and ++ indicate high frequency.

previously demonstrated that RTpiMi and RTdiMI cells consist of stem and progenitor cells, having potentially the ability to differentiate into goblet-like cell (Pasquariello et al., 2021), it is possible to infer that the mucosa-repairing cascade that characterizes the mouse intestine may have been triggered in RT cells by the prolonged exposure to IVD. The fact that the goblet-like cells found in the AV platform were positive for PAS staining suggests that an active mucin secretion is taking place. Their exclusive presence in the AV suggests that this platform better stimulates cellular differentiation.

Abundant PAS-positive supranuclear vacuoles (SNV) are commonly found in the distal intestine of several fish species, including RT (Verdile et al., 2020). Their presence has been related to the internalization of whole proteins (Debnath and Saikia, 2021) and to antigen sampling (Løkka and Koppang, 2016). Irrespective of their function, it is interesting to observe that IVD supplementation also induced the formation of structures with morphology, and affinity for PAS similar to SNV. Moreover, these were mainly located in RTdiMI cells underlying the difference between the two cell lines and the fact that they preserved the features of the respective intestinal tract of origin.

IVD at any concentration in both MMfb and AV induced the formation of a structure that looked like a basal membrane, a structure that acts as an anchorage site for epithelial cells and emphasizes a distinctive apical–basal polarity. *In vivo*, its formation is the result of the continuous bidirectional crosstalk between epithelial and mesenchymal cells, and both contribute to its secretion in a complementary manner (Simon-Assmann et al., 2010). The fact that a basal membrane was not observed in the TC platform, where exclusively epithelial cells were present, indicates that its formation depends specifically on the interactions between fibroblasts and epithelial cells and not from the prolonged exposure to IVD.

The exposure to IVD also strongly influenced the degree of enterocyte differentiation in the form of ALP activity. This aspect was influenced by the interaction between platform and cell line. ALP

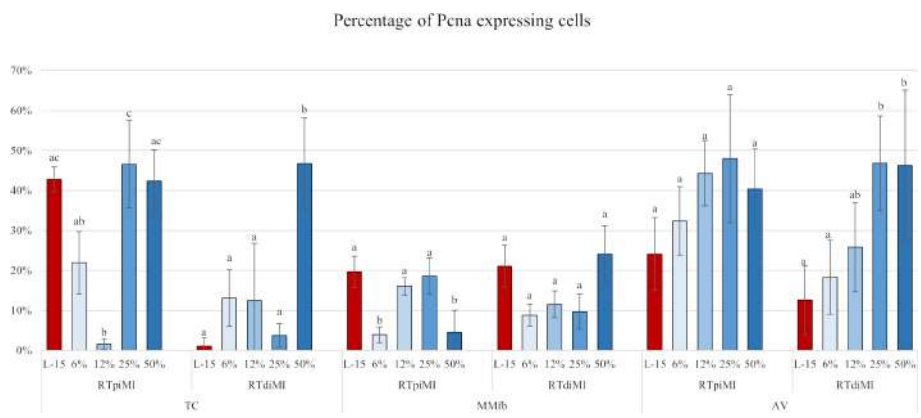

FIGURE 11
Bar charts showing the percentage of Pcna$^+$ cells compared to the total of epithelial cells quantified in RTpiMI and RTdiMI cultured in combination with TC, MMfb, and AV after 21 days of chronic exposure to increasing concentrations of IVD. Values are expressed as mean ± SD. Differences were considered statistically significant if $p < 0.05$. Different superscripts within the same culture conditions (platform and cell line) indicate statistically significant differences.

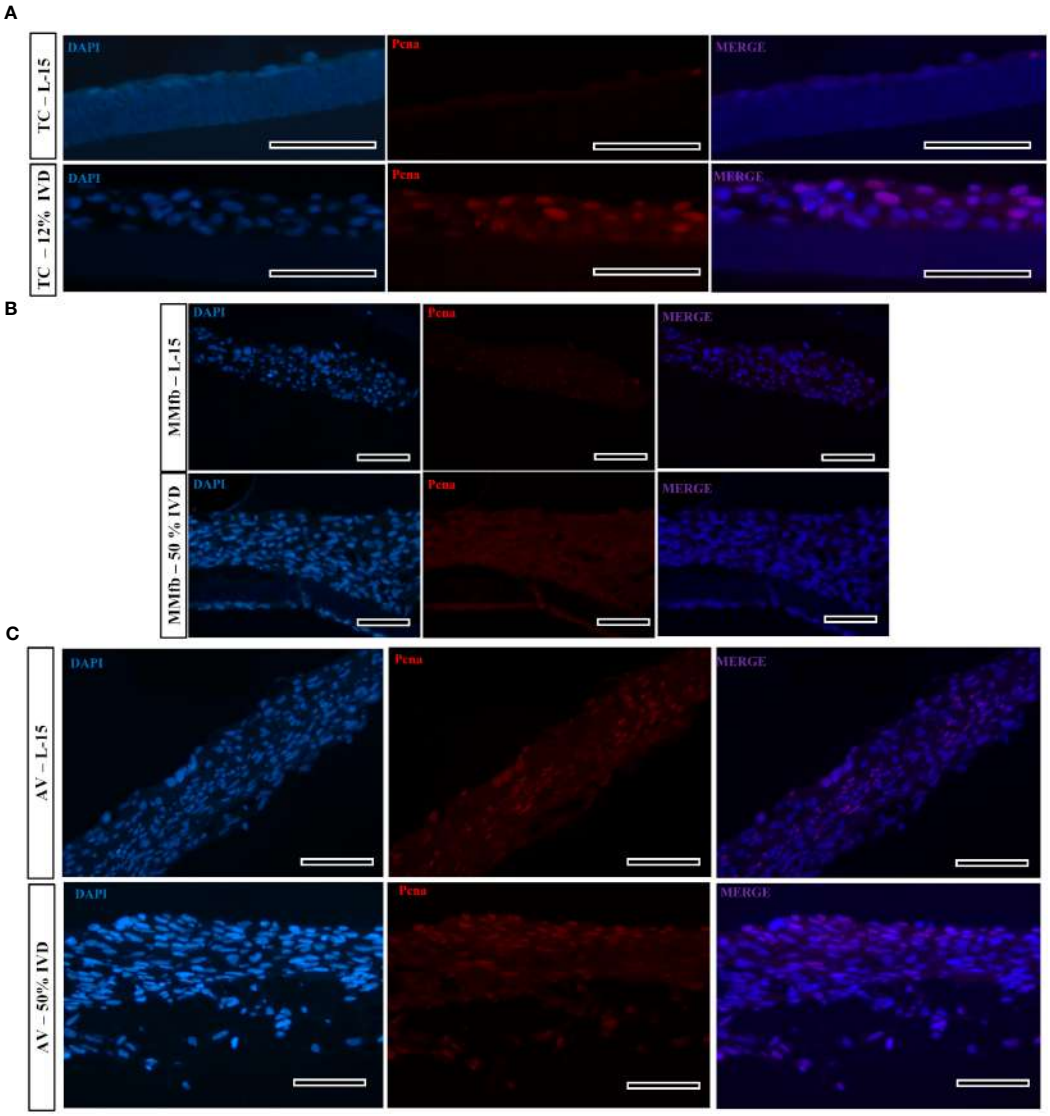

FIGURE 12
Representative images of proliferating cell nuclear antigen (Pcna—red signal) immunostaining in TC **(A)**, MMfb **(B)**, and AV **(C)** after 21 days of chronic exposure to IVD and in the respective controls. Pcna signal is restricted to the cell nuclei. Nuclei are counterstained with DAPI (blue signal) (scale bar, 50 µm).

activity completely disappeared in the MMfb, significantly decreased in the AV, but did not vary in TC, highlighting that the three platforms induced different responses to the IVD. Moreover, the fact that ALP activity did not always follow a dose-dependent pattern further confirms the different response elicited by the various combinations of cell lines and platforms. However, the significant reduction of enterocyte differentiation is consistent with our hypothesis that IVD induces a certain degree of enterocyte de-differentiation possibly followed by a differentiation towards the secretory lineages.

To verify whether the epithelial stratification correlated with a parallel increase in cell proliferation, we measured the number of $Pcna^+$ cells. Results were variable depending on the combinations of platform, cell line, and IVD concentrations. For instance, RTdiMI cells exposed to 50% IVD in TC and AV platforms induced a proliferative effect significantly higher than in the respective controls. In contrast, any IVD dose induced a significant increase in cell proliferation at the end of the experiment (day 21) in MMfb. A possible explanation could be that, while cells grown in TC and AV reached their TEER plateau on day 21, when the count has been performed, in MMfb, both lines reached their TEER plateau approximately at day 10 of culture. Therefore, it is possible that the intense proliferative activity that resulted in the epithelial stratification was already concluded by day 10 of culture. Further experiments will be required to optimize the different protocols for each platform.

Overall, our results highlight the suitability of the RT intestinal organotypic platforms to perform further functional studies aimed to predict intestinal permeability and/or absorption of nutrients and compounds through the barrier system. Among others, the bioavailability of small peptides and free amino acids represent an attractive target when evaluating the digestibility of novel feed combinations. Recently, we demonstrated that multiple variables (such as IVD concentration, length of the exposure, the different

epithelial cell lines, and the IVD diluent) have to be considered based on the final experiment goal (Pasquariello et al., 2023). We gained the necessary knowledge to assess the proteolytic activity of RT epithelial cells, to quantify the amount of single amino acids and their respective absorption rate using simple TC inserts. In our future experiments, the same paraments will be measured using cell-based organotypic platforms.

Conclusions

Our results indicate that the combinations between the two cell lines and the three platforms induced different responses to IVD exposure. For many of these responses, it is possible to find the correspondence with *in vivo* reactions, including the persistence of differences related to the origin of the cell lines from different tracts of the intestine. With regard to the platforms, overall, TC typically quenched most cell reactions, MMfb generated overly sensitive responses, while cells grown in the AV platform reacted with a dose–response effect for most parameters. This suggests that the AV platform may provide a more physiologically relevant response. However, further experiments are needed before a reliable conclusion can be reached on this point, possibly exposing the platforms to feeds with known contrasting digestibility and health effects.

Data availability statement

The raw data supporting the conclusions of this article will be made available by the authors, without undue reservation. The data presented in this study are openly available in the Fish-AI repository hosted at https://dataverse.unimi.it/dataverse/fish-AI (accessed on 10 July 2023).

Ethics statement

Ethical review and approval was not required for the study on animals in accordance with the local legislation and institutional requirements.

Author contributions

NV, FC, MC, RPas, and RPav performed the analysis; DP, RF, AT, TK, AB, TB, and FG contributed to conception and design of the study; NV and FG wrote the first draft of the manuscript; DP, RF, AT, TK, AB, TB, and FG were involved in writing, review, and editing; FG, funding acquisition. All authors contributed to manuscript revision, and read and approved the submitted version.

Funding

This work was supported by the European Union's Horizon 2020 research and innovation program under grant agreement No. 828835.

Acknowledgments

The authors acknowledge support from the University of Milan through the APC initiative. The authors are also grateful to Karina Koczberska and to Chiara Gatti for their help with morphological and functional analysis.

Conflict of interest

The authors declare that the research was conducted in the absence of any commercial or financial relationships that could be construed as a potential conflict of interest.

Publisher's note

References

Bednarek, R. (2022). *In vitro* methods for measuring the permeability of cell monolayers. *Methods Protoc.* 5 (1), 17. doi: 10.3390/mps5010017

Bell, J. G., Henderson, R. J., Tocher, D. R., and Sargent, J. R. (2004). Replacement of dietary fish oil with increasing levels of linseed oil: Modification of flesh fatty acid compositions in atlantic salmon (Salmo salar) using a fish oil finishing diet. *Lipids* 39, 223–232. doi: 10.1007/s11745-004-1223-5

Brodkorb, A., Egger, L., Alminger, M., Alvito, P., Assunção, R., Ballance, S., et al. (2019). INFOGEST static in *vitro* simulation of gastrointestinal food digestion. *Nat. Protoc.* 14, 991–1014. doi: 10.1038/s41596-018-0119-1

Caimi, C., Gasco, L., Biasato, I., Malfatto, V., Varello, K., Prearo, M., et al. (2020). Could dietary black soldier fly meal inclusion affect the liver and intestinal histological traits and the oxidative stress biomarkers of siberian sturgeon (Acipenser baerii) juveniles? *Animals* 10 (1), 155. doi: 10.3390/ani10010155

Cardinaletti, G., Marco, P., Daniso, E., Messina, M., Donadelli, V., Finoia, M. G., et al. (2022). Growth and welfare of rainbow trout (Oncorhynchus mykiss) in response to graded levels of insect and poultry by-product meals in fishmeal-free diets. *Animals* 12 (13), 1698. doi: 10.3390/ani12131698

Debnath, S., and Saikia, S. K. (2021). Absorption of protein in teleosts: a review. *Fish Physiol. Biochem.* 47, 313–326. doi: 10.1007/s10695-020-00913-6

Felix, K., Tobias, S., Jan, H., Nicolas, S., and Michael, M. (2021). Measurements of transepithelial electrical resistance (TEER) are affected by junctional length in immature epithelial monolayers. *Histochem. Cell Biol.* 156, 609–616. doi: 10.1007/s00418-021-02026-4

Ferruzza, S., Rossi, C., Scarino, M. L., and Sambuy, Y. (2012). A protocol for in *situ* enzyme assays to assess the differentiation of human intestinal Caco-2 cells. *Toxicol. Vitr.* 26, 1247–1251. doi: 10.1016/j.tiv.2011.11.007

Goswami, M., Yashwanth, B. S., Trudeau, V., and Lakra, W. S. (2022). Role and relevance of fish cell lines in advanced in *vitro* research. *Mol. Biol. Rep.* 49, 2393–2411. doi: 10.1007/s11033-021-06997-4

Jung, S. M., and Kim, S. (2022). *In vitro* models of the small intestine for studying intestinal diseases. *Front. Microbiol.* 12. doi: 10.3389/fmicb.2021.767038

Kawano, A., Haiduk, C., Schirmer, K., Hanner, R., Lee, L. E. J., Dixon, B., et al. (2011). Development of a rainbow trout intestinal epithelial cell line and its response to lipopolysaccharide. *Aquac. Nutr.* 17, e241–e252. doi: 10.1111/j.1365-2095.2010.00757.x

Kurashima, Y., Yamamoto, D., Nelson, S., Uematsu, S., Ernst, P. B., Nakayama, T., et al. (2017). Mucosal mesenchymal cells: Secondary barrier and peripheral educator for the gut immune system. *Front. Immunol.* 8. doi: 10.3389/fimmu.2017.01787

Løkka, G., Dhanasiri, A. K. S., Krogdahl, Å., and Kortner, T. M. (2022). Bile components affect the functions and transcriptome of the rainbow trout intestinal epithelial cell line RTgutGC. *Fish Shellfish Immunol.* 131, 1144–1156. doi: 10.1016/j.fsi.2022.10.049

Løkka, G., Gamil, A. A. A., and Evensen, Ø. (2023). Establishment of an in *vitro* model to study viral infections of the fish intestinal epithelium. *Cells* 12 (11), 1531. doi: 10.3390/cells12111531

Løkka, G., and Koppang, E. O. (2016). Antigen sampling in the fish intestine. *Dev. Comp. Immunol.* 64, 138–149. doi: 10.1016/j.dci.2016.02.014

Mahapatro, M., Foersch, S., Hefele, M., He, G. W., Giner-Ventura, E., Mchedlidze, T., et al. (2016). Programming of intestinal epithelial differentiation by IL-33 derived from pericryptal fibroblasts in response to systemic infection. *Cell Rep.* 15, 1743–1756. doi: 10.1016/j.celrep.2016.04.049

Minghetti, M., Drieschner, C., Bramaz, N., Schug, H., and Schirmer, K. (2017). A fish intestinal epithelial barrier model established from the rainbow trout (Oncorhynchus mykiss) cell line, RTgutGC. *Cell Biol. Toxicol.* 33, 539–555. doi: 10.1007/s10565-017-9385-x

Pasquariello, R., Pavlovic, R., Chacon, M. A., Camin, F., Verdile, N., Panseri, S., et al. (2023). Development of a Rainbow Trout (Oncorhynchus mykiss) Intestinal *In vitro* Platform for Profiling Amino Acid Digestion and Absorption of a Complete Diet. *Animals* 13 (14), 2278. doi: 10.3390/ani13142278

Pasquariello, R., Verdile, N., Pavlovic, R., Panseri, S., Schirmer, K., Brevini, T. A. L., et al. (2021). New Stable Cell Lines Derived from the Proximal and Distal Intestine of Rainbow Trout (Oncorhynchus mykiss) Retain Several Properties Observed in *vivo*. *Cells* 10 (6), 1555. doi: 10.3390/cells10061555

Randazzo, B., Zarantoniello, M., Gioacchini, G., Cardinaletti, G., Belloni, A., Giorgini, E., et al. (2021). Physiological response of rainbow trout (Oncorhynchus mykiss) to graded levels of Hermetia illucens or poultry by-product meals as single or combined substitute ingredients to dietary plant proteins. *Aquaculture* 538, 736550. doi: 10.1016/j.aquaculture.2021.736550

Schneider, C. A., Rasband, W. S., and Eliceiri, K. W. (2012). NIH Image to ImageJ: 25 years of image analysis. *Nat. Methods* 9, 671–675. doi: 10.1038/nmeth.2089

Simon-Assmann, P., Spenle, C., Lefebvre, O., and and Kedinger, M. (2010). Chapter 8 – the role of the basement membrane as a modulator of intestinal epithelial–mesenchymal interactions. Ed. K. H. Kaestner. *Prog. Mol. Biol. Transl. Sci.* 96, 175–206. doi: 10.1016/B978-0-12-381280-3.00008-7

Verdile, N., Camin, F., Pavlovic, R., Pasquariello, R., Stuknytė, M., De Noni, I., et al. (2023). Distinct organotypic platforms modulate rainbow trout (Oncorhynchus mykiss) intestinal cell differentiation in *vitro*. *Cells* 12, 1843. doi: 10.3390/cells12141843

Verdile, N., Cardinaletti, G., Faccenda, F., Brevini, T. A. L., Gandolfi, F., and Tibaldi, E. (2022). Ectopic stem cell niches sustain rainbow trout (Oncorhynchus mykiss) intestine absorptive capacity when challenged with a plant protein-rich diet. *Aquaculture* 564, 739031. doi: 10.1016/j.aquaculture.2022.739031

Verdile, N., Pasquariello, R., Scolari, M., Scirè, G., Brevini, T. A. L., and Gandolfi, F. (2020). A detailed study of rainbow trout (Onchorhynchus mykiss) intestine revealed that digestive and absorptive functions are not linearly distributed along its length. *Animals* 10, 745. doi: 10.3390/ani10040745

Wang, J., Lei, P., Gamil, A. A. A., Lagos, L., Yue, Y., Schirmer, K., et al. (2019). Rainbow trout (Oncorhynchus mykiss) intestinal epithelial cells as a model for studying gut immune function and effects of functional feed ingredients. *Front. Immunol.* 10. doi: 10.3389/fimmu.2019.00152